



HAL
open science

Residence time distribution analysis in the transport and compressing screws of a biomass pretreatment process

Kevin Lachin, Ziad Youssef, Giana Almeida, Patrick Perre, Denis Flick

► To cite this version:

Kevin Lachin, Ziad Youssef, Giana Almeida, Patrick Perre, Denis Flick. Residence time distribution analysis in the transport and compressing screws of a biomass pretreatment process. *Chemical Engineering Research and Design*, 2020, 154, pp.162-170. 10.1016/j.cherd.2019.12.011 . hal-03140277

HAL Id: hal-03140277

<https://hal.science/hal-03140277>

Submitted on 14 Apr 2022

HAL is a multi-disciplinary open access archive for the deposit and dissemination of scientific research documents, whether they are published or not. The documents may come from teaching and research institutions in France or abroad, or from public or private research centers.

L'archive ouverte pluridisciplinaire **HAL**, est destinée au dépôt et à la diffusion de documents scientifiques de niveau recherche, publiés ou non, émanant des établissements d'enseignement et de recherche français ou étrangers, des laboratoires publics ou privés.

Residence time distribution analysis in the transport and compressing screws of a biomass pretreatment process

Kevin LACHIN*, Ziad YOUSSEF*, Giana ALMEIDA*, Patrick PERRE** and Denis FLICK*.

* Université Paris-Saclay, INRAE, AgroParisTech, UMR SayFood, 91300, Massy, France.

** LGPM, Laboratoire de Génie des Procédés et Matériaux, CentraleSupélec, Université Paris-Saclay, 3 rue Joliot Curie, 91192 Gif-sur-Yvette, France

Abstract

The raise of environmental concerns in the past decades consequently increased the need of obtaining cleaner sources of energy. Among the studied alternatives, second generation biofuels (produced from non-food resources) are one of the most promising solutions and nearly reached industrialization. The production of cellulosic bioethanol is one of the possibilities of second generation biofuels, and the studies involving the use of cellulosic compounds to produce bioethanol recently increased. Its production involves four dependent steps: pretreatment, enzymatic hydrolysis, fermentation and distillation. This work considered the pretreatment stage, aiming at modifying the structure of the lignocellulosic biomass so that cellulose becomes more accessible to enzymatic hydrolysis step.

This work particularly focused on the biomass flow characterization in the transport and compression screws involved in the pretreatment step of an industrial-scale process. The main challenge was firstly to perform measurements on an industrial-scale device working under harsh conditions. Residence time distribution (RTD) experiments were thus performed using a novel methodology adapted to these working conditions. Sodium carbonate was selected as a tracer. Due to the reaction with the acidified biomass, both electrical conductivity and pH were monitored at the exit of the screws. A chemical model was developed, allowing the determination of tracer concentrations from the measured data. The measurements obtained were compared with three optimized models: a combination of plug flow and continuous stirred tank reactor in series (PFR-CSTR), plug flow with axial dispersion (AD) and a model based on the Zusatz function. The results of this work pointed out the non-plug flow behavior of these screws in their standard working conditions. In accordance with the physical motion of the tracer inside the screws, the use of the PF-CSTR is recommended for representing RTD inside screws in conditions in which backflow is likely to occur.

Keywords: biomass, lignocellulose, bioethanol, biofuel, screws, residence time distribution, residence time distribution modelling.

Nomenclature

a	Zusatz function parameter (s^{-1})
b	Zusatz function parameter (s)
c	Zusatz function parameter (-)
\dot{m}	Mass flow rate ($kg \cdot s^{-1}$)
\dot{V}	Volumetric flow rate ($m^3 \cdot s^{-1}$)
$[x]$	Concentration of x ($mol \cdot m^{-3}$)
M	Molecular weight ($kg \cdot mol^{-1}$)
m	Mass of injected tracer (kg)
E	Residence time distribution function (s^{-1})
S	Normalized concentration of Na^+ (s^{-1})
t	Time (s)
-	
\bar{t}	Mean residence time (s)
-	
\bar{t}_{CSTR}	Mean residence time in the CSTR (s)
t_{PF}	Residence time in the PFR (s)
t_{step}	Tracer injection time into the pilot (s)
$t_{aqueous\ flow}$	Average exit time of the aqueous flow (s)
t_{belt}	Average exit time out of the grade conveyor belt (s)
$t_{screws\ first\ exit}$	First exit time of the aqueous flow (s)
λ_t	Measured electrical conductivity ($mS \cdot m^{-1}$)
λ_x^m	Molar (electrical) conductivity of x ($mS \cdot m^2 \cdot mol^{-1}$)
θ	Dimensionless time (-)

Abbreviation

<i>RTD</i>	Residence Time Distribution
<i>PFR</i>	Plug Flow Reactor
<i>CSTR</i>	Continuous Flow Stirred Tank Reactor
<i>AD</i>	Axial Dispersion

1. Introduction

The dramatic increase in the worldwide population during the last decades (more than 50% in the last 30 years) raised several questions in the scientific community about the way to feed these populations, their impact on the environment (soil pollution, global warming...) but also the sustainability of the current energy supplies in regards with our way of life. As the fossil fuels resources are expected to last for approximately 100 more years, there is a real urge to massively produce renewable, cost-effective, environmental-friendly sources of energy. Among the studied options (solar, wind...), biofuels are considered as one of the most promising alternatives. We can currently distinguish between four generations of biofuels, depending on the type of feedstock used for its production. The first generation is produced from agricultural crops, and thus raises legitimate questions regarding the competition with food production. Second generation biofuels, obtained from the conversion of lignocellulosic compounds like agricultural wastes, straw ... thus gained very high interest.

The general process of second generation bioethanol production from ground biomass is summarized in *Fig. 1*. Four main steps are involved: biomass pretreatment, enzymatic hydrolysis, fermentation and distillation. The step of interest in this study is the pretreatment stage. Its main purpose is to modify the cellulosic biomass structure so that cellulose can become accessible to perform enzymatic hydrolysis [1]. The pretreatment step is thus crucial to the overall bioethanol production process as it will directly affects the efficiency of the subsequent steps. For this reason, several treatments were studied in the literature: chemical (acid hydrolysis, ionic liquids use...), physical chemical (steam explosion, ammonia fiber explosion...) and mechanical (milling). Extensive information about the pros and cons of each technique can easily be found in the literature [2,3]. In the studied process, a diluted acid hydrolysis at high temperature is performed. The biomass is firstly acidified, then conveyed to a cooking reactor inducing a modification of the size and structure of the acidified biomass. This pretreatment step can be subdivided into three separate parts:

- The biomass impregnation with an adequate pretreating agent (Part 1);
- The transportation and compression inside a succession of screws (Part 2) ;
- The biomass cooking inside a dedicated reactor (Part 3).

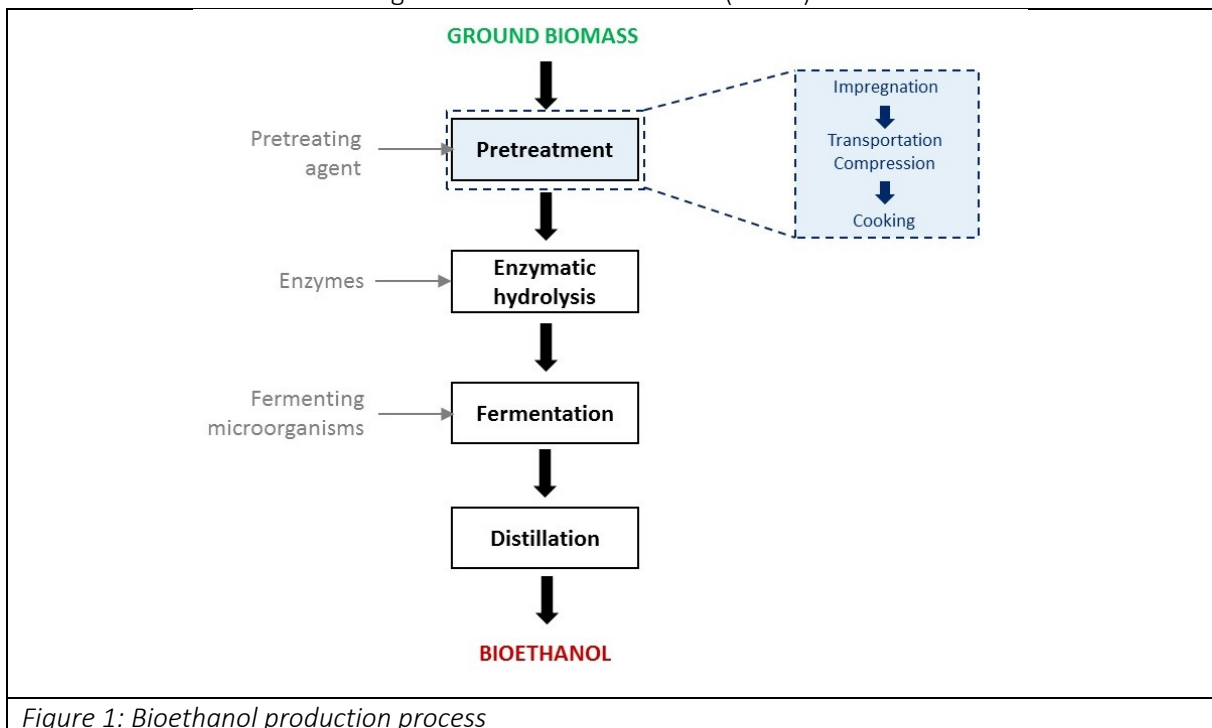


Figure 1: Bioethanol production process

As Part 2 and 3 of the pretreatment step involve product transportation and transformation through a series of screws, a comprehensive hydrodynamic investigation is needed for these steps. Part 2 (transportation, compression) is far from being anecdotal: the compression screw indeed creates a security seal that prevents the vapour water steam used in the cooking step from leaving the cooking reactor through the screws. The compression screw also dehumidifies the biomass before entering the reactor, thus reducing the steam amount needed to increase the product temperature in the cooking reactor. The flow understanding of this succession of screws is thus essential as they play a key role in the pretreatment process. It has to be noted that the flow inside the cooking part (Part 3) of this specific process was comprehensively studied in a previous article [4]: consequently, this article solely focuses on the Part 2 of the pretreatment step.

Introduced by Dankwerts [5], the Residence Time Distribution (RTD) function E is of great help to evaluate the flow behavior of a continuous process and its mixing performances. Also, RTD can be very useful to predict the hydrodynamics when scaling-up the process and determining optimal process working conditions. Its estimation is thus essential for an extensive continuous process study and hydrodynamic characterization. In regards with with RTD in screw and extrusion devices, the works so far published mainly concerns the fields of bioenergies and food production. Recently, Chamberlain et al. [6] studied the residence time distribution of wood chips inside a torrefier reactor incorporating a screw reactor. Nachenius et al [7] worked on the residence time distribution of coarse particles (air-dried pine chips, dehulled rice and quarts sand) in a rotating screw conveyor reactor and proposed a suited mathematical model. Both the authors managed to found increasing differences between the theoretical residence time and the mean residence time of the experimental distribution with increasing degree of filling. Among the interesting studies on the topic, Sievers et al. [8], recently worked on the residence time distribution of an horizontal auger tube reactor aimed at pretreating biomass (here hammer milled corn stover) using NaCl as a tracer. The authors pointed out that no liquid/solid stratification was noticed during the tests, making NaCl an acceptable tracer for pretreating biomass. Bi and Jiang [9] used both numerical modelling and experimental approach to study the residence time distribution inside a single screw pin barrel. Other RTD studies [10–12] can also be found for twin screw systems used for extrusion or granulation purposes. All these works found that the mean experimental residence time of these screws was larger than the theoretical one expected from the screw rotation speed, thus giving interest to residence time experiments and modelling in these systems.

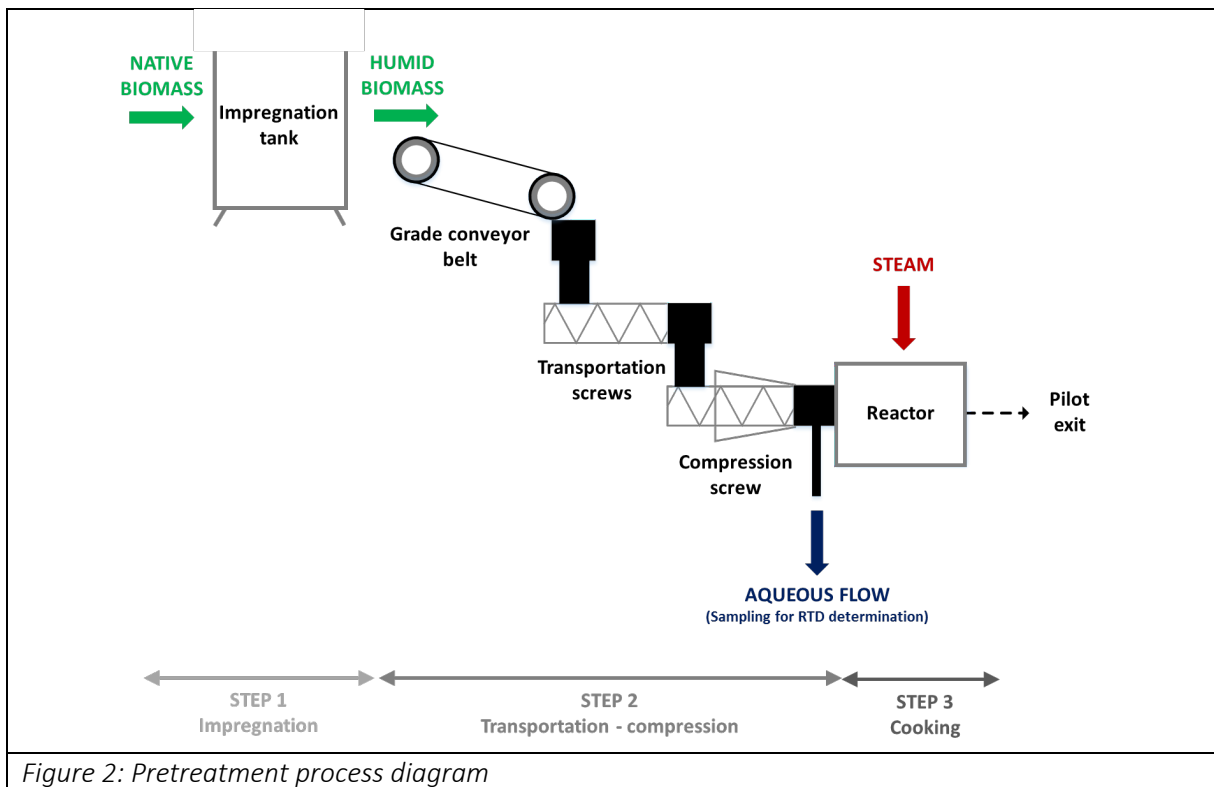
This paper focuses on the residence time distribution in the transport and compression screws during the pretreatment of wheat straw through the use of a novel methodology adapted to strongly acidic working conditions (pH lower than 2). Sodium carbonate (Na_2CO_3) was used as a tracer and as it reacts with the biomass, both the pH and the electrical conductivity were measured at the exit of the screws. These measurements afterwards allowed the determination of the tracer concentration (sodium ion) so that residence time distribution function could be obtained. It has to be noted that the use of this inexpensive and non-toxic tracer for lignocellulosic biomass is to the best of our knowledge rather new as the only work using it for that purpose was very recently published in a previous work published by Youssef et al. [4]. This previous study also showed that this tracer is adapted to harsh thermodynamic conditions (temperature around 200°C, pressure up to 23 bar) that can be found in industrial biomass pretreatment reactors. Unlike most of the tracers used for RTD experiments, sodium carbonate reacts with the acid medium, explaining the need of monitoring both pH and electrical conductivity. The novelty of this work is thus to apply this RTD determination methodology to the transportation and compression screws of an industrial-size biomass pretreatment process. As massive quantities of product are required to perform these trials, the fact that the same harmless and non-expensive methodology than for the biomass pretreatment reactor can be used for these devices is of great help for designing optimal experimental trials without any useless biomass waste and handling risks. This work thus provides important knowledge about the granular flow in these screws and ultimately allows a better understanding of the pretreatment process at industrial scale that can be used for further unit operation sizing.

2. Material and methods

The native biomass used in this study is composed of ground wheat straw (approximately 20 mm length) cultivated in the Pomacle region (France) in 2014.

2.1 Industrial pretreatment process

The industrial pretreatment process used in this study is presented in *Fig. 2*.



The acid impregnation of the native biomass (*Step 1*) was carried out inside 1 m³ containers stored at atmospheric pressure. During this step, diluted aqueous solution of sulfuric acid (between 0.5 and 1% w/w) was put in contact with the biomass during 20 hours at room temperature. The liquid phase was afterwards flushed using a dedicated valve. The result of the impregnation can be observed in *Fig. 3*.



Figure 3: Wheat straw after acid impregnation

The treated biomass was then injected in the process using a grade conveyor belt, feeding the transport and compression screws (Step 2). While the two first screws are dedicated to the transportation, the third one compresses the biomass to dehumidify it before entering the reactor. This last screw is of prime importance in the process as it also creates a seal that avoid steam from leaving the reactor through the screws. At the exit of the compression screw, the biomass loses most of its water before entering to the cooking reactor (Step 3). This water aqueous flow thus exits the pretreatment process, allowing the monitoring of the pH and conductivity. These measurements can then be used for the determination of RTD for the entirety of the screw set (transportation and compression).

2.2 Choice of the tracer

In order to perform a relevant RTD study, an appropriate inert tracer has to be carefully chosen. Some guidelines are to be followed in order to select an appropriate tracer:

- Easy to detect while used in small amounts;
- Not easily degraded, especially under high temperature and pressure conditions;
- Should not have an impact on the rheological properties of the carrier fluid;
- Should faithfully follow the fluid motion.

In case of industrial-scale trials, salt tracers can be considered as they are relatively cheap, have little environmental impact and can be supplied in large amounts. In this study, sodium carbonate was selected, mostly because it comes with small risks on humans and no corrosion with stainless steel, even at high temperatures. More details about the tracer selection can be found in a previous work [4]. However, the main drawback is its reaction with sulfuric acid, which has to be taken into account by measuring both pH and conductivity.

2.3 Measurement accuracy

2.3.1 Conductivity measurement

The conductivity of the outlet aqueous solution was measured through the use of a conductivity meter (Sension + EC5, Hach) allowing measurement of ionic conductivities in aqueous solution even under tough thermodynamic conditions in acid medium. This device can measure conductivities from $1\mu\text{S}\cdot\text{cm}^{-1}$ to $1\text{S}\cdot\text{cm}^{-1}$ with an accuracy of 0.5% of the measurement range.

2.3.2 pH measurement

pH was monitored using a portable pH-meter (HI 98128, Hanna) measuring values ranging from 0.1 to 13.9. Once calibrated, the measurement accuracy was 0.01 pH unit.

2.4 Operating procedure

2.4.1 Preparation of the traced biomass

It was experimentally found that the optimal tracer mass fraction in the native biomass to perform RTD experiments is around 6% w/w. Traced biomass was thus prepared by mixing 10 kg of biomass (previously impregnated with acid) with 600 g of tracer, to reach a tracer mass fraction of 5.7% w/w.

2.4.2 Tracer introduction

The biomass was introduced into the pretreatment process by the means of the grade conveyor belt. As the pilot works with industrial-scale quantities, one issue is to obtain a perfect entrance signal. It was chosen to inject the traced biomass as a step of duration $t_{step} = 69$ s. To do so, knowing the speed of the

belt, two marks were done at the corresponding distance. When the steady state in the pretreatment process (screws and cooking reactor) was reached (more details given in [4]), the traced biomass was evenly reparted between the marks, ensuring a perfect crenel signal at the inlet of the first transportation screw. The measurement beginning ($t=0$) corresponds to the moment the first particle of traced biomass is introduced into the first screw. It also has to be noted that the traced and untraced biomass initially had the same acid fraction.

2.4.3 Conductivity and pH measurements

The electrical conductivity and pH measurements were performed on the aqueous flow at the exit of the compression screw. The pH was directly measured at the outlet while the conductivity measurements were afterwards performed on samples collected every 10 s.

3. Theory

3.1 Tracer concentration modelling

In most of the practical cases, RTD function determination is performed in systems where the conductivity of the carrier medium can be neglected and where the salt tracer does not reacts with the carrier medium. Consequently, only the tracer conductivity is measured. It is then possible to quickly access the tracer concentration through the knowledge of the conductivity with an adequate calibration. In this study however, several ionic species are natively present in the treated biomass. It was thus chosen to consider the sodium ion Na^+ as the traced specie as it does not reacts with the species in solution and is not initially present in the treated biomass.

The general reaction of carbonate sodium with sulfuric acid is depicted by *Eq. 1*:



The reaction products are sodium sulfate, liquid water and vapor carbon dioxide. Using this chemical reaction, it is then possible to develop a chemical model (details are given in [4]) allowing the calculation of the sodium ion concentration in the flow $[Na^+]_t$ as a function of the pH and the electrical conductivity. The expression obtained is detailed in *Eq. 2*.

$[Na^+]_t = \frac{\lambda_t - \lambda_{NB} - \frac{\lambda^*}{2\lambda_{H_3O^+}^m + \lambda_{SO_4^{2-}}^m} \cdot \left[(10^{pH^* - pH_t} - 1) \cdot \lambda_{CO_3^{2-}}^m + (2 \cdot 10^{pH^* - pH_t}) \cdot \lambda_{H_3O^+}^m + \lambda_{SO_4^{2-}}^m \right]}{\lambda_{Na^+}^m + 0.5\lambda_{CO_3^{2-}}^m}$	<i>Eq. 2</i>
---	--------------

pH^* and λ^* stands for the pH and conductivity of the acidified biomass without tracer. λ_t , λ_{NB} and λ_i^m respectively denotes the conductivity of the solution at the exit of the process, the native biomass conductivity (non acidified) and the molar conductivity of the i compound.

Knowing $[Na^+]_t$ at the outlet ($[Na^+]_{out,t}$), it is then possible to calculate the normalized signal at the outlet S_{out} using *Eq. 3*:

$S_{out}(t) = \frac{[Na^+]_{out,t}}{\int_0^\infty [Na^+]_{out,t} \cdot dt}$	<i>Eq. 3</i>
---	--------------

It has to be noted that S_{out} is equal to E , the RTD function only in the case of an impulse (or Dirac function) injection. In the most general case, S_{out} and E are related to the normalized signal at the inlet, S_{in} , through the convolution integral expressed by Eq. 4.

$S_{out}(t) = \int_0^t S_{in}(t').E(t - t').dt'$	Eq. 4
--	-------

In this study, the inlet signal is a crenel function of duration t_{step} . The normalized inlet signal can thus be explained as depicted by Eq. 5.

$\begin{aligned} t \leq t_{step} : S_{in}(t) &= 1/t_{step} \\ t > t_{step} : S_{in}(t) &= 0 \end{aligned}$	Eq. 5
--	-------

Assuming an analytical solution for E with fitting parameters, it is possible to fully determine E by minimizing the difference between the calculated and experimental results. When E is obtained, the mean residence time of the distribution \bar{t} can be determined by calculating the first order moment of E [13,14] as described by Eq. 6.

$\bar{t} = \int_0^{\infty} t.E(t).dt$	Eq. 6
---------------------------------------	-------

3.2 RTD function determination

When it comes to conventional chemical reactors, four main types of models are commonly used to characterize flow behavior: Plug Flow Reactor (PFR), Continuous Flow Stirred Tank Reactor (CSTR), Axial Dispersion model (AD) and non-ideal reactor models obtained combining the three above-mentioned flow models [15]. Danckwerts described the plug flow reactor as a behavior representing elements of fluid entering the reactor at the exact same time, and moving with constant and equal velocity by using parallel paths to leave the reactor at the same time. The CSTR model was described by the same author as being a behavior occurring when the fluid inside the considered reactor is perfectly mixed, thus having its properties uniform and equal to those of the outlet flow. CSTR and PFR are thus ideal cases: the real behavior of a reactor is often likely to be between these two extremes. In the case of RTD of material flow in devices involving screws (screw conveyors, extruders), the AD model and PF-CSTR combination can be extensively found in the literature. Also, a third model, involving an empirical function called the Zusatz function was used by several authors. The sections below thus give extensive details on these approaches.

3.2.1 Axial dispersion modelling (AD)

The RTD modelling considering axial dispersion model is based on the 1-D convection-diffusion equation. The dispersion coefficient D_{ax} introduced encompasses all the transport phenomena except convection, meaning molecular diffusion, non-uniformity of the flow profile on a reactor section, turbulence... This coefficient is typically used to calculate the Peclet number Pe that compares the characteristic time by axial dispersion transportation and the characteristic time by convection transportation. The clear physical meaning of these parameters is one of the main strengths of this modelling approach, that has been widely used in solid units operations [16]. For an open-open reactor, this convection-diffusion equation can be analytically solved so that the RTD function E is expressed by Eq. 7.

$E(t) = \frac{1}{2} \cdot \sqrt{\frac{Pe}{\pi \cdot t \cdot \bar{t}_{AD}}} \cdot e^{\left(\frac{-Pe \cdot (\bar{t}_{AD} - t)^2}{4 \cdot t \cdot \bar{t}_{AD}}\right)}$	Eq. 7
--	-------

\bar{t}_{AD} here stands for the mean residence time obtained with Axial Dispersion modelling. In this study, \bar{t}_{AD} and Pe are the fitting parameters of this model.

3.2.2 Plug Flow – Continuous Flow Stirred Tank Reactor modelling (PF-CSTR)

The non-ideality of flow behavior in a real reactor can also be modelled by combining ideal reactor in series, as for example plug flow and continuous flow stirred tank reactors [17]. The simplest approach considers a CSTR without dead volume. It is however possible to modify the CSTR modelling by introducing a dead zone volume that cross-flows with the CSTR when significant material backflow is expected. This approach was proposed by Yeh et al. [18] in the case of a single screw extrusion process and afterwards used by other authors [19,20] for extrusion processes. In this study, we will focus on a simpler PF-CSTR modelling with no dead zone. This modelling strategy was considered by several authors in the case of screw processes, especially extruders [19,21]. The time spent in the plug flow reactor (corresponding to the time at the outlet without any signal increase) is here denoted by t_{PF} , whereas the mean residence time of the CSTR is named \bar{t}_{CSTR} . For this modelling, the RTD function can be expressed by Eq. 8 while the mean total time $\bar{t}_{PF-CSTR}$ is obtained through Eq. 9.

$\begin{aligned} t \leq t_{PF} : E(t) &= 0 \\ t > t_{PF} : E(t) &= \frac{1}{\bar{t}_{CSTR}} \cdot e^{-\left(\frac{t-t_{PF}}{\bar{t}_{CSTR}}\right)} \end{aligned}$	Eq. 8
--	-------

$\bar{t}_{PF-CSTR} = t_{PF} + \bar{t}_{CSTR}$	Eq. 9
---	-------

In the case of a PF-CSTR model, using the definition of the convolution integral (Eq. 4) and the analytical form of the RTD function (Eq. 8), it is thus possible to propose the following analytical solution for S_{out} (Eq. 10):

$\begin{aligned} t \leq t_{PF} : S_{out}(t) &= 0 \\ t_{PF} < t \leq t_{PF} + t_{step} : S_{out}(t) &= \frac{1}{t_{step}} \cdot \left[1 - e^{-\left(\frac{t-t_{PF}}{\bar{t}_{CSTR}}\right)} \right] \\ t > t_{PF} + t_{step} : S_{out}(t) &= \frac{1}{t_{step}} \cdot \left[e^{-\left(\frac{t-(t_{PF}+t_{step})}{\bar{t}_{CSTR}}\right)} - e^{-\left(\frac{t-t_{PF}}{\bar{t}_{CSTR}}\right)} \right] \end{aligned}$	Eq. 10
--	--------

The model is subsequently adjusted to the experimental data by adjusting the values of t_{PF} and \bar{t}_{CSTR} .

3.2.3 Zusatz modelling

In the extrusion process field, an empirical modelling approach for E was proposed by Zusatz [22] and successfully used in several extrusion studies [9,23–25] (Eq. 11).

$E(t) = a \cdot \left(\frac{b}{t}\right)^{c+1} \cdot \exp \left[\left(\left(\frac{b}{t}\right)^c - 1 \right) \cdot \left(\frac{-c-1}{c} \right) \right]$	Eq. 11
---	--------

The Zusatz function, established using extrusion experimental data, depends on a set of three parameters to be fitted: a , b and c . The parameter a can be seen as a scaling parameter of the RTD curve while b directly depends on the mean residence time. So far, c was found no physical meaning. Contrary to the other approaches presented, this model does not rely on a strong physical ground, but on empirical results: its limitations are therefore so far unknown [25].

3.2.4 Determination of the fitting parameters

All the model optimizations presented in this study were performed using the software MATLAB® (vers. R2015a). For each model, the corresponding RTD function (Eq. 7, 8 and 11 respectively for the AD modelling, PF-CSTR modelling and Zusatz modelling) was used with the convolution integral introduced in Eq. 4 to calculate the outlet normalized signal $S_{out,calc}$. For the PF-CSTR model, a direct analytical solution was used (Eq. 10) while for the two other models, the convolution integral was estimated using the *integral* function of the software. The values of the fitting parameters were then estimated by minimizing the sum of the squared differences between the measured and calculated values of S_{out} through the use of the *fminsearch* function.

4. Results and discussion

4.1 Operating conditions

The experiments were performed on an industrial-scale installation. As a consequence, only the usual working conditions of the screws (one set of screw speeds) were investigated, with two tests (Test 1 and Test 2) performed on wheat straw to ensure repeatability. The native biomass had an initial acid content below 1% w/w. For the two experiments, the tracer concentration was equal to 5.6% w/w.

4.2 Na⁺ concentration

According to Eq. 2, $[Na^+]_{out,t}$ was calculated using both the pH and electrical conductivity measurements performed on the aqueous outlet flow obtained from the compression screw.

4.2.1 Native biomass conductivity

The native biomass electrical conductivity was measured and found to be $\lambda_{NB} = 123 \mu\text{S}\cdot\text{cm}^{-1}$. This measurement was performed in the exact same conditions as for the outlet flow. Four ionic compounds are found in the measured solutions: Na^+ , CO_3^{2-} , SO_4^{2-} and H_3O^+ . The molar conductivities of these ions at 25°C are given in Table 1 [26].

Table 1: Molar conductivities of Na^+ , CO_3^{2-} , SO_4^{2-} and H_3O^+ at 25°C

Ion	Molar conductivity (S.m ² .mol ⁻¹)
Na^+	5.0
CO_3^{2-}	13.9
SO_4^{2-}	16.0
H_3O^+	35.0

4.2.2 Raw measurements and Na⁺ concentration

The results of the pH and conductivity measurements performed at the outlet of the pretreatment screws (Test 1 and Test 2) are presented in *Fig. 4*. For all the subsequent graphs, a dimensionless time θ is introduced so that:

$\theta = \frac{t}{t_{step}}$	<i>Eq. 12</i>
-------------------------------	---------------

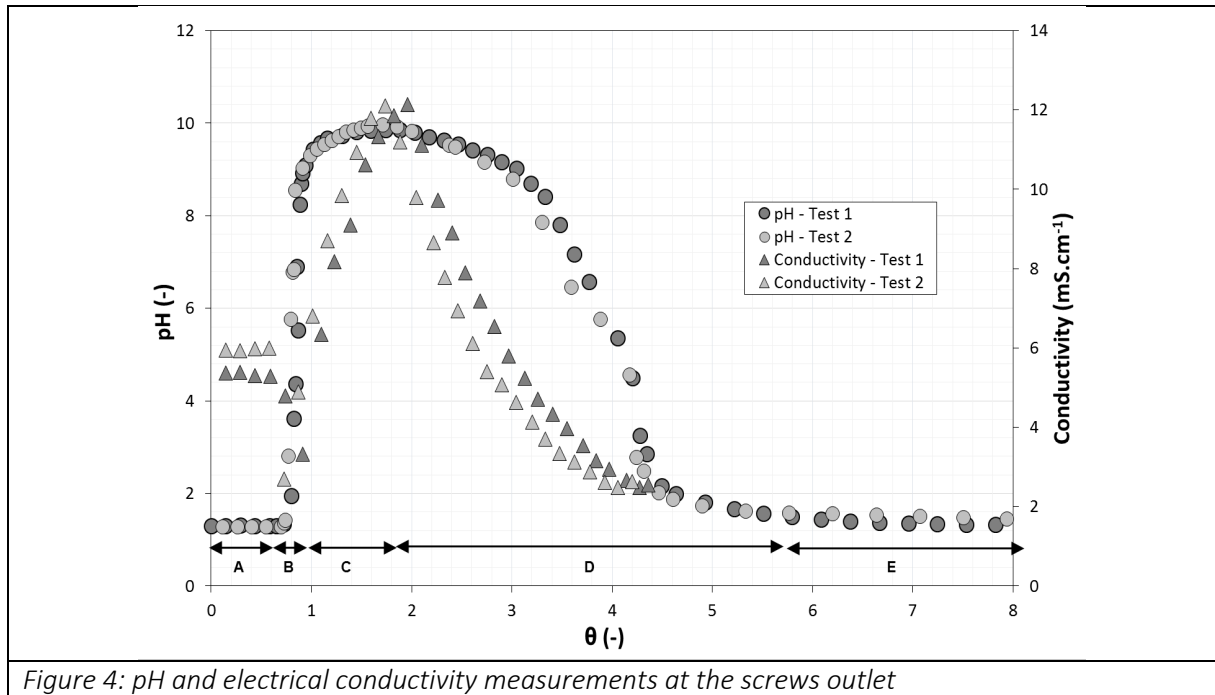


Figure 4: pH and electrical conductivity measurements at the screws outlet

The first observation is that the curves of Tests 1 and 2 obtained for both the pH and the conductivity are almost similar, thus ensuring repeatability of the measurements. At the beginning (A), no tracer is detected. Consequently, both the pH and the conductivity of the outlet stream are almost constant. This stream is mainly composed from water and acid coming from the biomass pretreatment, explaining the rather low pH obtained (around 1.3). When the first tracer molecules are detected (B, appearing at $\theta = 0.7$), the pH start to increase, however the conductivity decreases. Qualitatively speaking, as the hydroxide ion concentration diminish while reacting with the carbonate ion, the pH increases and the total conductivity decreases due to the difference between the molar conductivity of H_3O^+ and Na^+ . When the tracer is in excess (C), the pH will only present a slight evolution (up to around 9.9), however the conductivity will naturally increase until a maximum value around 12.1 mS.cm^{-1} , directly related to the maximum tracer concentration induced by the residence time distribution. A decrease in both pH and conductivity is afterwards obtained (D), directly linked to the tracer concentration decrease due to the hydrodynamics inside the process, and the initial value of the pH is reached from around $\theta = 5.8$, indicating that a large majority of the initial tracer was flushed out of the system.

Using *Eq.2*, it is then possible to calculate the Na^+ concentration in the outlet flow using the pH and electrical conductivity measurements earlier obtained. The results obtained for the two tests performed are presented in *Fig.5*. As the raw measurements were rather similar, the sodium ion concentration is unsurprisingly repeatable through the two performed tests. The obtained curves indeed displays the same concentration distribution shape and a peak of equal magnitude at approximately $\theta = 1.9$.

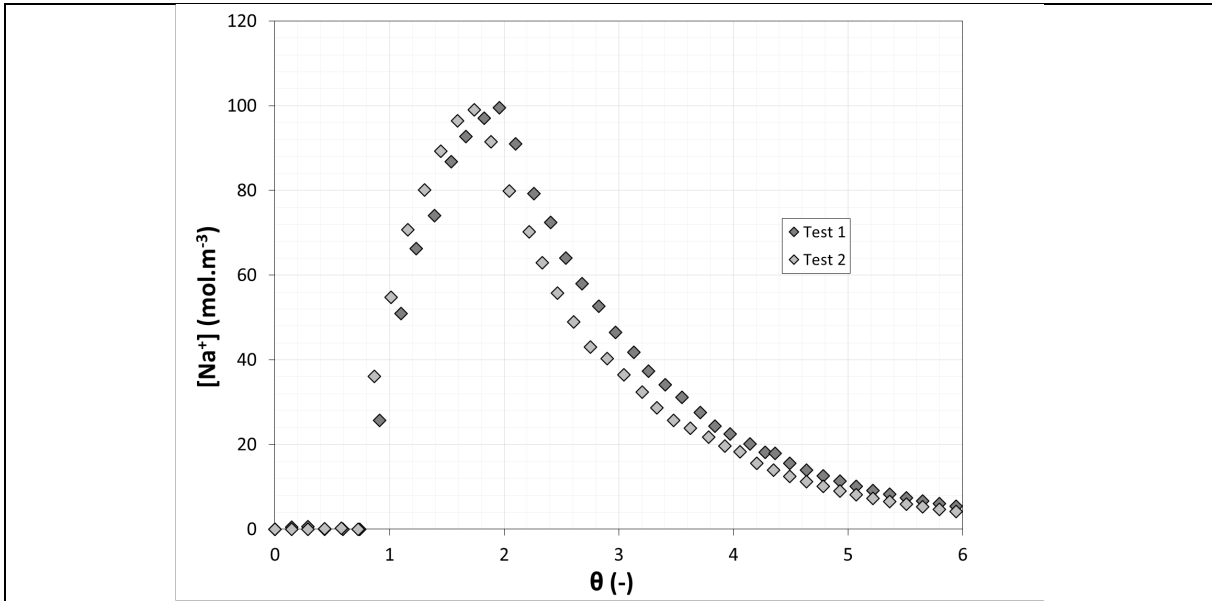


Figure 5: Evolution of the sodium ion concentration in the outlet stream through time

4.3 Residence Time Distribution functions

4.3.1 Experimental signal data

Once $[Na^+]$ calculated, it is possible to access the normalized signal at the outlet using Eq.3. Integration is performed through a trapezoidal numerical integration using the experimental data (*trapz* MATLAB function). The results obtained are presented in Fig. 6. The inlet normalized signal (a crenel function of duration t_{step} and height $1/t_{step}$) is also represented in the figure. As the tracer is introduced under a solid state, this signal was not directly measured, however reasonably assumed to be a perfect crenel (see 2.4.2).

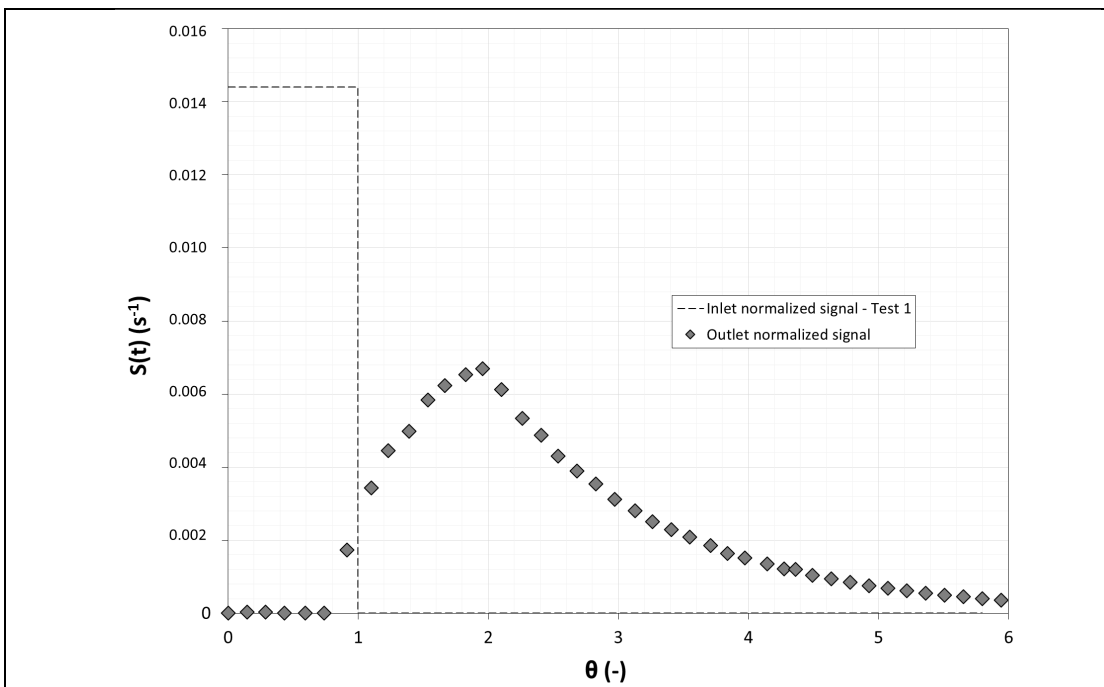


Figure 6: Evolution of the outlet normalized signal through time

Using this data, it is then possible to calculate the parameters of the RTD functions. The parameters are estimated minimizing the root mean square error (RMSE) which characterizes the difference between the calculated signal ($S_{out,calc}$) and the measured one (S_{out}) over the n experimental points (Least-Squares method, Eq. 13).

$$RMSE = \left(\sum_{i=1}^n (S_{out,calc}(i) - S_{out}(i))^2 / n \right)^{1/2} \quad \text{Eq. 13}$$

4.3.2 RTD functions determination

For all the subsequent graphs, only Test 1 is displayed for concisions concerns. Using the above-mentioned method, the parameters are fitted for the three models considered in the study. The optimized parameters are presented in Table 2, Table 3 and Table 4.

Table 2: Optimized parameters for the AD model

	$Pe (-)$	$\bar{t}_{AD} (s)$	$RMSE (s^{-1})$	$\bar{t}/t_{th} (-)$
Test 1	5.4	99.5	$3.0 \cdot 10^{-4}$	195 %
Test 2	4.8	86.8	$4.3 \cdot 10^{-4}$	176 %

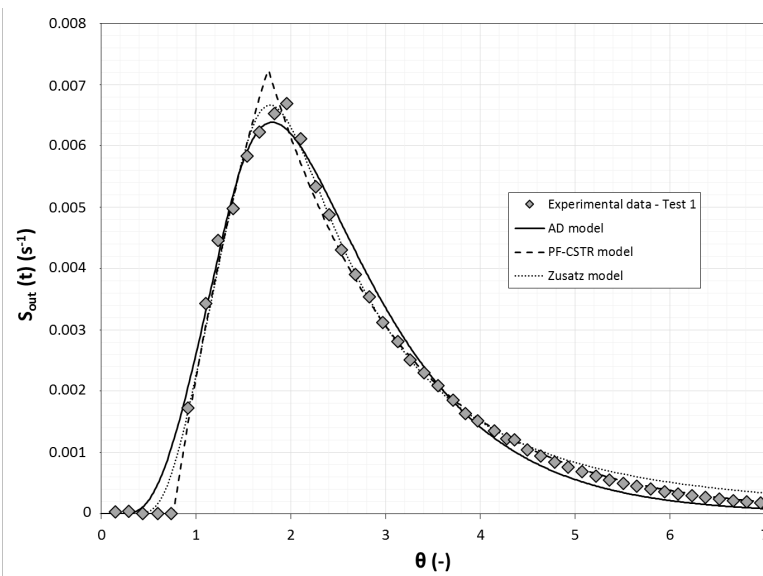
Table 3: Optimized parameters for the PF-CSTR model

	$t_{PF} (s)$	$\bar{t}_{CSTR} (s)$	$RMSE (s^{-1})$	$\bar{t}/t_{th} (-)$
Test 1	52.4	99.3	$2.1 \cdot 10^{-4}$	217 %
Test 2	44.9	89.8	$2.4 \cdot 10^{-4}$	192 %

Table 4: Optimized parameters for the Zusatz model

	a	b	c	RMSE (s^{-1})	\bar{t}/t_{th} (-)
Test 1	$7.5 \cdot 10^{-3}$	77.7	1.6	$1.9 \cdot 10^{-4}$	352%
Test 2	$8.3 \cdot 10^{-3}$	66.6	1.6	$2.9 \cdot 10^{-4}$	316%

A



B

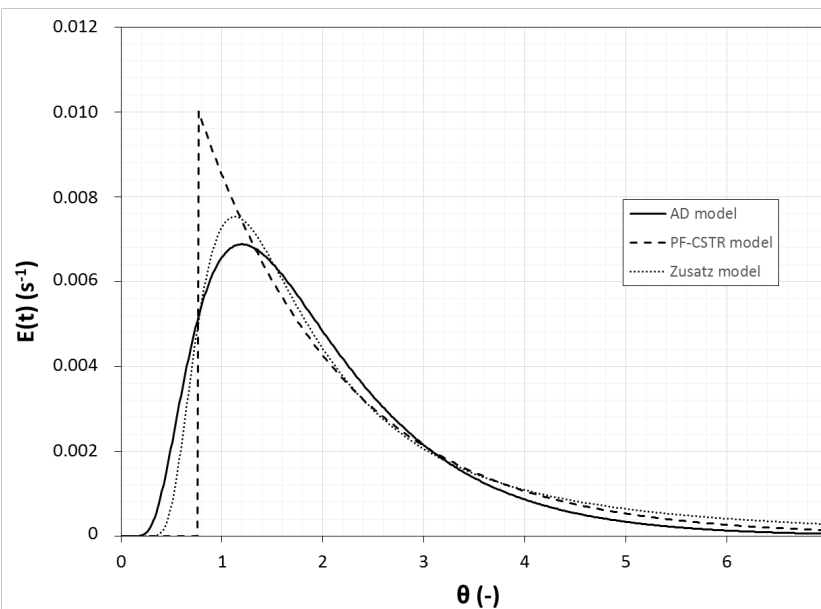


Figure 7: Experimental and calculated values of S_{out} (A) and E (B) using the PF-CSTR, AD and Zusatz models

The graphical representation of the optimal modelled output signals is presented in Fig. 7.A, and the corresponding RTD functions (Eq. 7, 8 and 11) in Fig 7.B. From these elements, several comments can

be made. Firstly, at the chosen working conditions, the transportation and compression screws display a highly non-ideal behaviour, notably observed by the very low Pe values (inferior to 6, while a plug-flow is reasonably assumed over 100) obtained with the optimized model. While the PF-CSTR model faithfully depicts the trends of the experimental signal, the AD model is physically more questionable as an increase in signal is observed at approximately $\theta = 0.3$, compared to the experimental value around 0.7. The same observation can also be formulated for the optimized Zusatz model, starting to increase around $\theta = 0.4$. The least-squares values furthermore validate this qualitative observation, with RMSE values systematically lower for the PF-CSTR model than for the AD, thus indicating a better model adequation with the experimental data. Concerning the RMSE values obtained with the Zusatz model, we can observe that they lie in the same order of magnitude than for the PF-CSTR model, especially for Test 1. However, we graphically observe that at long enough times ($\theta > 5$), the Zusatz model optimized in this study overestimates the output signal, resulting in estimated mean residence times significantly higher than the ones obtained with the two other models. Consequently, the Zusatz model can hardly be recommended here.

When looking at *Table 3*, we observe significant differences between the theoretical residence time inside the screws (calculated from the geometrical properties of the screws and the rotation speed) and the mean residence time obtained through the RTD function (*Eq. 5*), respectively 217 and 192% for Test 1 and Test 2. While these differences may appear surprisingly high, such discrepancies are expected in screws conveyors. Several studies [6,7,27] indeed reported differences of that order of magnitude that can be ascribed to the degree of filling of the screw conveyor. Indeed, on one hand, between the rotating screws and the shell, there is a slight clearance space in which the product is moving slower. On the other hand, when the degree of filling is high enough, material slipping from one screw pitch to the subsequent one is expected, thus drastically increasing the residence time inside the reactor.

The AD model, involving both tracer diffusion upwards and backwards is here not suited to the motion of the tracer inside the conveyor. The Zusatz model, while presenting a fairly good adequation to the experimental data, is suspected to overestimate the output signal on the long times, and consequently the mean residence time. Assuming the outlet signal is mainly due to the hydrodynamics inside the transportation screws (which is coherent with the small theoretical residence time inside the compression screw in regards to the transportation ones) and the material is perfectly stirred inside each pitch, the PF-CSTR model makes physically sense and is much more recommended when representing RTD inside screws where backflow is likely to have a significant impact on the residence time.

5. Conclusion

As industrial-scale biomass pretreatment installations are currently under development to produce 2nd generation biofuel, methodologies suited to the harsh conditions encountered in these processes have to be proposed to obtain reliable data. This study focused on obtaining the residence time distribution function in the transport and compression screws of an industrial biomass pretreatment process in conventional working conditions. Due to the large quantities handled and the rough conditions to be undergone in the overall pretreatment process, the selection of an adequate tracer was of prime importance. The choice made in this study was to use sodium carbonate, a cheap, harmless and non-corrosive tracer. As the tracer reacts with the acidified biomass, a chemical model was developed to calculate the sodium ion concentration from the pH and molar conductivity of the outlet flow. These measurements were thus experimentally performed to ultimately determine the signal response to a crenel inlet function. The RTD was modelled using three approaches: a conventional AD model, a PF-CSTR model and a model based on the Zusatz function. The results obtained clearly underlined the non-plug flow behavior of the process in its standard working conditions, supposedly due to the material

backflow that can occur in these devices under moderate to high screw degree of filling. Under these physical considerations, the PF-CSTR appeared to be the most suited of these models to describe the RTD inside this device at the studied working conditions.

By proposing an approach based on a straightforward RTD modelling and the use of a cheap tracer adapted to harsh conditions, this study ultimately provides a novel and efficient methodology to study RTD inside industrial screw conveyors. This work can furthermore be used for better sizing and conception of pretreatment screws for biofuels applications, or other processes involving lignocellulosic biomass.

References

- [1] N. Mosier, Features of promising technologies for pretreatment of lignocellulosic biomass, *Bioresource Technology*. 96 (2005) 673–686.
- [2] P.F.H. Harmsen, W. Huijgen, L. Bermudez, R. Bakker, Literature review of physical and chemical pretreatment processes for lignocellulosic biomass, Wageningen : Wageningen UR Food & Biobased Research, 2010.
- [3] A. García, M. González Alriols, J. Labidi, Evaluation of different lignocellulosic raw materials as potential alternative feedstocks in biorefinery processes, *Industrial Crops and Products*. 53 (2014) 102–110.
- [4] Z. Youssef, F. Ducept, H. Bennaceur, B. Malinowska, G. Almeida, P. Perre, D. Flick, Residence time distribution in a biomass pretreatment reactor: Experimentation and modeling, *Chemical Engineering Research and Design*. 125 (2017) 233–244.
- [5] P.V. Danckwerts, Continuous flow systems. Distribution of residence times: P. V. Danckwerts, *Chem. Engng Sci.* 2: 1–13, 1953, *Chemical Engineering Science*. 50 (1995) 3855.
- [6] C. Chamberlin, D. Carter, A. Jacobson, Measuring residence time distributions of wood chips in a screw conveyor reactor, *Fuel Processing Technology*. 178 (2018) 271–282.
- [7] R.W. Nachenius, T.A. van de Wardt, F. Ronsse, W. Prins, Residence time distributions of coarse biomass particles in a screw conveyor reactor, *Fuel Processing Technology*. 130 (2015) 87–95.
- [8] D.A. Sievers, E.M. Kuhn, J.J. Stickel, M.P. Tucker, E.J. Wolfrum, Online residence time distribution measurement of thermochemical biomass pretreatment reactors, *Chemical Engineering Science*. 140 (2016) 330–336.
- [9] C. Bi, B. Jiang, Study of residence time distribution in a reciprocating single-screw pin-barrel extruder, *Journal of Materials Processing Technology*. 209 (2009) 4147–4153.
- [10] J. Gao, G.C. Walsh, D. Bigio, R.M. Briber, M.D. Wetzel, Residence-time distribution model for twin-screw extruders, *AIChE Journal*. 45 (2004) 2541–2549.
- [11] A. Kumar, J. Vercruyssen, V. Vanhoorne, M. Toiviainen, P.-E. Panouillot, M. Juuti, C. Vervaet, J.P. Remon, K.V. Gernaey, T.D. Beer, I. Nopens, Conceptual framework for model-based analysis of residence time distribution in twin-screw granulation, *European Journal of Pharmaceutical Sciences*. 71 (2015) 25–34.
- [12] S.M. Lee, J.C. Park, S.M. Lee, Y.J. Ahn, J.W. Lee, In-line measurement of residence time distribution in twin-screw extruder using non-destructive ultrasound, *Chemical Engineering Science*. 17 (2005) 9.
- [13] R. Andreux, G. Petit, M. Hemati, O. Simonin, Hydrodynamic and solid residence time distribution in a circulating fluidized bed: Experimental and 3D computational study, *Chemical Engineering and Processing: Process Intensification*. 47 (2008) 463–473.
- [14] K. Smolders, J. Baeyens, Overall solids movement and solids residence time distribution in a CFB-riser, *Chemical Engineering Science*. 55 (2000) 4101–4116.
- [15] M.E. Davis, R.J. Davis, *Fundamentals of chemical reaction engineering*, International ed, McGraw-Hill, Boston, 2003.
- [16] Y. Gao, F.J. Muzzio, M.G. Ierapetritou, A review of the Residence Time Distribution (RTD) applications in solid unit operations, *Powder Technology*. 228 (2012) 416–423.

- [17] D. Wolf, W. Resnick, Residence Time Distribution in Real Systems, *Industrial & Engineering Chemistry Fundamentals*. 2 (1963) 287–293.
- [18] A.-I. Yeh, Y.-M. Jaw, Modeling residence time distributions for single screw extrusion process, *Journal of Food Engineering*. 35 (1998) 211–232.
- [19] M. Seker, Residence time distributions of starch with high moisture content in a single-screw extruder, *Journal of Food Engineering*. 67 (2005) 317–324.
- [20] C. Nikitine, E. Rodier, M. Sauceau, J. Fages, Residence time distribution of a pharmaceutical grade polymer melt in a single screw extrusion process, *Chemical Engineering Research and Design*. 87 (2009) 809–816.
- [21] D. Wolf, D.H. White, Experimental study of the residence time distribution in plasticating screw extruders, *AIChE Journal*. 22 (1976) 122–131.
- [22] B. Zusatz, PhD dissertation, Université Louis Pasteur, 2001.
- [23] A. Poulesquen, B. Vergnes, P. Cassagnau, A. Michel, O.S. Carneiro, J.A. Covas, A study of residence time distribution in co-rotating twin-screw extruders. Part II: Experimental validation, *Polymer Engineering & Science*. 43 (2003) 1849–1862.
- [24] X. Zhang, L. Feng, S. Hoppe, G. Hu, Local residence time, residence revolution, and residence volume distributions in twin-screw extruders, *Polymer Engineering & Science*. 48 (2008) 19–28.
- [25] J. Wesholowski, H. Podhaisky, M. Thommes, Comparison of residence time models for pharmaceutical twin-screw-extrusion processes, *Powder Technology*. 341 (2019) 85–93.
- [26] P. Vanýsek, D.R. Lide, *CRC Handbook of Chemistry and Physics*, CRC Press, 2006.
- [27] S.S. Waje, A.K. Patel, B.N. Thorat, A.S. Mujumdar, Study of Residence Time Distribution in a Pilot-Scale Screw Conveyor Dryer, *Drying Technology*. 25 (2007) 249–259.